# AIRBORNE HIGH-RESOLUTION DIGITAL IMAGING SYSTEM

Prado-Molina, J.[1], Peralta-Higuera,A.[1], Palacio-Prieto, J.L. [1] & Sandoval R. [2].

[1]Instituto de Geografía, UNAM. Circ. Ext. Cd. Universitaria, Coyoacán 04510. México D.F. México. jprado@igg.unam.mx, aperalta@igg.unam.mx, palacio@servidor.unam.mx
[2]Facultad de Ingeniería, UNAM, Cd. Universitaria Coyoacán, 04510, México D.F. México. rafael@seguridad.fi-a.unam.mx

*Received: January 6th, 2004. Accepted: December 15th, 2005*

ABSTRACT

A low-cost airborne digital imaging system capable to perform aerial surveys with small-format cameras is introduced. The equipment is intended to obtain high-resolution multispectral digital photographs constituting so a viable alternative to conventional aerial photography and satellite imagery. Monitoring software handles all the procedures involved in image acquisition, including flight planning, real-time graphics for aircraft position updating in a mobile map, and supervises the main variables engaged in the imaging process. This software also creates files with the geographical position of the central point of every image, and the flight path followed by the aircraft during the entire survey. The cameras are mounted on a three-axis stabilized platform. A set of inertial sensors determines platform's deviations independently from the aircraft and an automatic control system keeps the cameras at a continuous nadir pointing and heading, with a precision better than ± 1 arc-degree in three-axis. The control system is also in charge of saving the platform's orientation angles when the monitoring software triggers the camera. These external orientation parameters, together with a procedure for camera calibration give the essential elements for image orthocorrection. Orthomosaics are constructed using commercial GIS software.

This system demonstrates the feasibility of large area coverage in a practical and economical way using small-format cameras. Monitoring and automatization reduce the work while increasing the quality and the amount of useful images.

RESUMEN

Se presenta un sistema de adquisición de imágenes aéreas digitales de bajo costo, capaz de llevar a cabo levantamientos aéreos con cámaras de formato pequeño. Este equipo obtiene fotografías digitales multiespectrales de alta resolución, constituyendo una alternativa viable a la fotografía aérea convencional y a las imágenes de satélite. Un programa de monitoreo maneja todos los procedimientos involucrados en la adquisición de las imágenes, incluyendo la planeación del vuelo, la graficación en tiempo real de la posición de la aeronave, en un mapa móvil, y el monitoreo de las principales variables comprometidas en el proceso de obtención de imágenes. Este programa también crea archivos con la posición geográfica del centro de cada imagen y de la trayectoria de vuelo seguida por la aeronave durante todo el levantamiento. Las cámaras están montadas en una plataforma estabilizada en tres ejes. Un conjunto de sensores inerciales, determina las desviaciones de la plataforma de manera independiente de la nave y un sistema de control automático mantiene las cámaras apuntando de manera continua hacia nadir con un rumbo fijo y con una precisión mejor que ± 1 grado en los tres ejes. El sistema de control también está a cargo de guardar los ángulos de orientación de la plataforma, en el momento en que el programa de monitoreo dispara la cámara. Éstos parámetros de orientación externa, junto con un procedimiento para calibrar la cámara, proporcionan los elementos esenciales para ortocorregir las imágenes. Los ortomosaicos son construidos mediante la utilización de programas comerciales de SIG.

Este sistema demuestra la factibilidad de poder llevar a cabo levantamientos aéreos en amplias zonas, de una manera práctica y económica, con cámaras de formato pequeño. El monitoreo y la automatización reducen el trabajo, mientras que la calidad y la cantidad de imágenes útiles, se incrementa considerablemente.

KEYWORDS: Airborne Stabilized Platform, Small-format Digital Cameras, Mobile Map, Drift-free IMU, Camera Calibration, Multispectral Digital Photography, Orthophotomap.

## 1. INTRODUCTION

Nowadays, the benefits obtained through image acquisition and interpretation, are evident. Utilization of satellite, and aerial imagery is of common practice for remote sensing applications in diverse areas, such as: meteorology, agriculture, disaster assessment, ecology, hydrology, forestry, etc., only to mention some of them. Over the last fifteen years, interest in the use of video [1,2], and small-format digital photography [3,4,5] as alternative remote sensing tools, was growing within photogrammetric researchers. Several efforts were made to introduce the CCD-based digital camera technology into the airborne commercial mapping and scientific research environment [6,7]. This newly developed tool begun with a digital camera used in stand-alone mode [8,9], and a first effort was focused on using it as a component of an integrated camera/GPS/INS system [10]. Airborne digital multispectral imaging systems are cost-effective well-established tools for collecting remotely sensed high-resolution imagery (i.e. pixel size ranges from 0.05 to 1.5 [m] depending on the project).

Technology advances are working in benefit of these systems, small (i.e. 16 Mpixels) to medium-format (i.e. 22 Mpixels) digital cameras increase the advantages of its utilization; resolution is always growing while the cost is maintained. Personal computers are also augmenting their capabilities allowing for faster and better management of all of the procedures involved in image acquisition and post-processing analysis. GPS receivers, key hardware components, are evolving in the same way, and commercial software for orthophoto production is also offered at competitive costs. Image availability, and the possibility of controlling spectral and spatial resolution are among the most important factors for the utilization of these airborne systems [2,6,7]; composed mosaics of color-IR imagery of flooded or damaged areas can be obtained within hours [11]. Despite higher resolution satellite imagery is now available (0.6 [m]), it often takes weeks to collect the area of interest, and even then the final geometric accuracy is only a few meters, at best. Hence aerial imagery is really the only way of meeting the high resolution, accuracy and quick delivery times being demanded [12]. To deal with these requirements, system's automatization is imperative to facilitate the work involved in handling all the procedures for digital mapping, from flight planning to mosaic construction [11].

Of paramount importance to the success of an airborne digital image survey is the correction of the imagery for geometric distortions, these are the displacements of imaged points from their expected locations and can be attributed to platform tilt at the time of image acquisition, inherent perspective distortion, lens distortion, and relief displacement. Correction of these errors (rectification) produces an orthographic projection of the imagery, an orthoimage [13]. Thus, the exterior orientation (i.e. three coordinates of the perspective center, and three rotation angles), the camera calibration (i.e. the lens distortion characteristics, the focal length, and principal point location), at least 3 ground control points and a digital terrain model, are indispensable for orthoimage generation. In the next paragraphs a system for airborne image acquisition, georeferencing, and orthorectified map production is presented, and at the end of the document its perspectives of utilization and limitations are identified.

## 2. OVERVIEW OF THE IMAGING SYSTEM

The monitoring software is in charge of image acquisition, and data storage using a mobile map as a navigation aid [14]. Camera calibration and distortion removal were implemented making use of adapted traditional laboratory methods [15]. Image orthocorrection as well as mosaic formation, has been performed with the usage of commercial software. A stabilized platform was designed and constructed for vertical photography acquisition, reducing significatively deformations introduced into the images by involuntary rotations of the aircraft [16]. More important in

this context, is the attitude determination system (ADS); in this particular application implemented by a two-axis (pitch and roll) vertical IMU, and an electronic compass for independent yaw determination [17]. The ADS is capable of obtaining platform orientation 12 times per second and its priority is to save the 3 attitude angles (exterior orientation), at the moment the camera is taking the picture, even if the control system became obliterated by excessive perturbations [17]. The positions are acquired with DGPS at 20 [Hz] and the solutions obtained in post processing, considering antenna displacements. Figure 1 shows a block diagram with the main components of the imaging system.

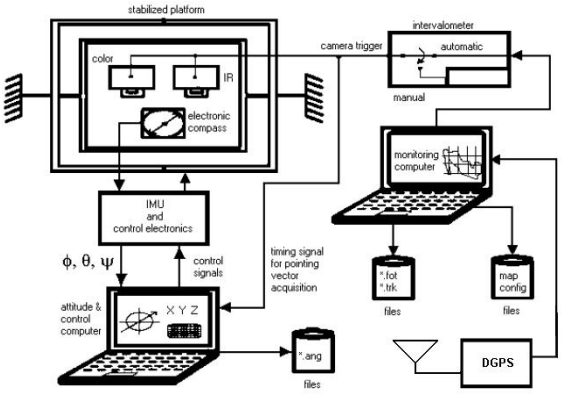


*Figure 1 Block diagram of the high-resolution digital imaging system.*

The arrangement described on this paper is an economical, and practical alternative for airborne high-resolution digital imaging, representing 5 to 10 percent of the cost of a conventional aerial photographic system [11,17]. It has been used in many research projects (e.g. [18,19,20,21]) and the utilization of the digital imagery in the context of a geographical information system (GIS) has proved to be very convenient for many land use management and monitoring applications.

## 3. SYSTEM DESCRIPTION

The imaging system (see figure 2) is composed by the monitoring, and the attitude determination and control subsystems. For simplicity each part will be explained separately, in fact, the only interaction between them is the sharing of the signal for camera triggering; when it occurs, the platform's attitude of this particular image, is saved in a *.ANG file. The monitoring system saves the *.FOT and *.TRK files, which corresponds to the geographical coordinates of the central point of every image, and the flight path followed by the aircraft during the entire survey, respectively [22]. This system can also operate in manual mode: the intervalometer can be used as an elementary backup camera-triggering device.

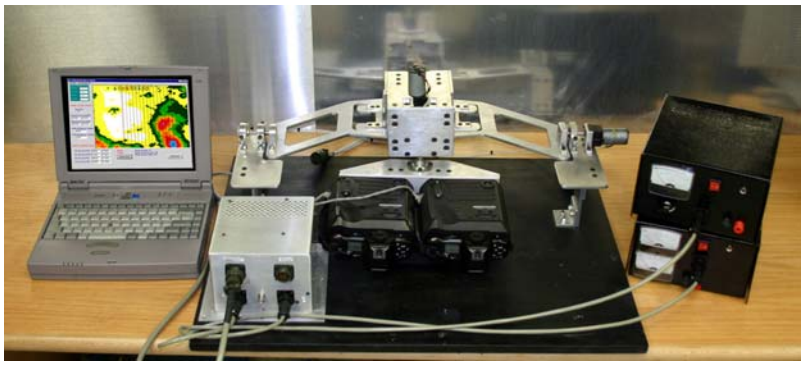

*Figure 2. Monitoring computer, inertial measurement unit, stabilized platform with two small-format cameras mounted, and power supplies.*

### 3.1 Monitoring system

This specifically designed software, written in Visual Basic[23], runs on a laptop computer over Windows® environment. The routine of configuration and initial data capturing is in charge to obtain all the required information to perform the flight planning. It is necessary to fill the blanks for: input port selection and baud rate for the GPS, the filenames for the *.FOT and *.TRK archives, the number of pixels in each row of the CCD camera, the airplane's velocity, the longitudinal and lateral overlapping, the pixel resolution in meters, and the number of images that each disk can handle (if not an USB port directly connected to the hard disc exists). This last parameter is indispensable to avoid image loosening, due to different disk storage capacities and image quality settings on the camera. If during the survey one or more parameters have to be changed (due to intense air traffic or climatic conditions, etc.), the program is able to recalculate a new scenario very quickly.

The map configuration routine is shown on figure 3. A digital map of the zone that will be covered can be loaded as a graphical navigation aid. This map can be obtained from scanned cartography, satellite imagery, digital elevation models, etc. The flight lines are outlined automatically over the digital map, once the UTM zone and the four corners of the area under study are entered. The total number of flight lines, images per line, and the total amount of photographs is then calculated and displayed.

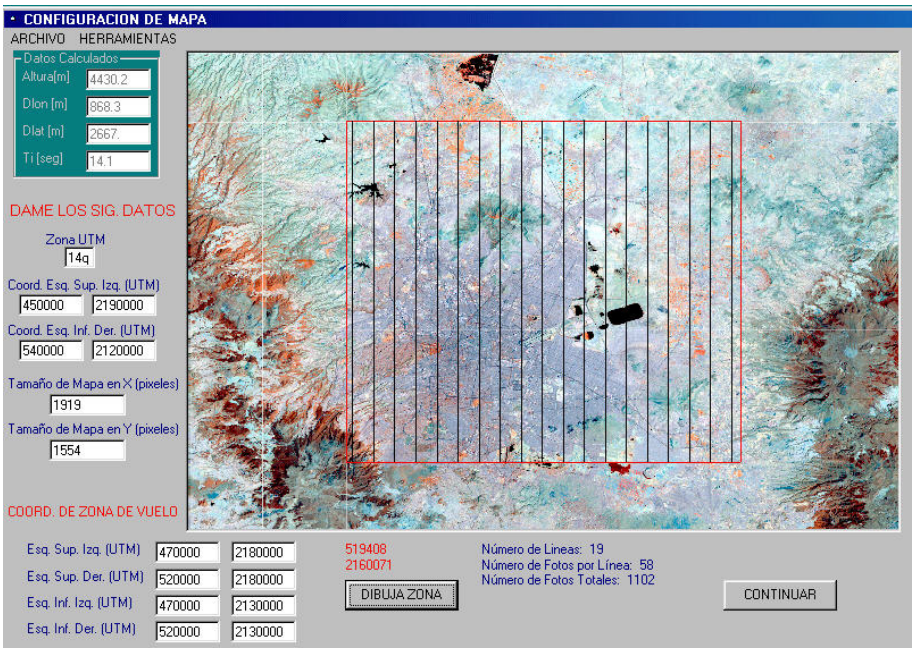


*Figure 3. Flight lines outlined over the digital map of the zone under study.*

Finally, the *flight mode* routine performs the most critical part of digital aerial photography acquisition. The most important variables are continuously monitored and their status accordingly displayed. In this operational mode the software updates the aircraft position every second, through the GPS receiver. DGPS solution [24] is obtained in post-processing with a data-logging interval of 20 [Hz]. The mobile map moves over the screen with the purpose to remain centered following the current position of the aircraft. A general drawing of the zone depicts the already flown lines and those remaining uncovered. Heading, speed (in knots, km/h and m/s), UTM coordinates of the current position, height, GPS active, and camera shutter, are also showed. Any problem detected by the navigator or the camera operator can be immediately solved with the lost of only a small number of frames, a 360° turn will allow finding the missed line again to capture out-of-track, non-recorded images, or those with too much inclination. This avoids the necessity to come back to the zone, for line repetitions with the economical consequences this implies. Figure 4 shows all the above-mentioned parameters.

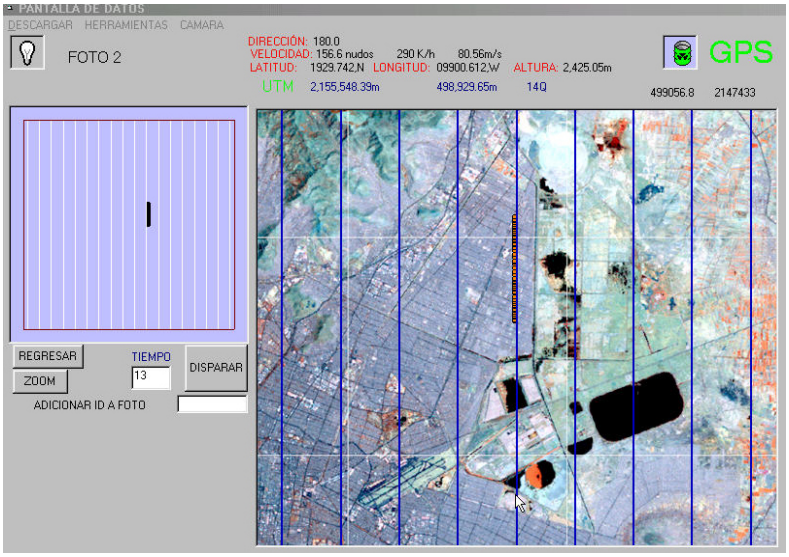


*Figure 4. Flight mode screen and data storage.*

3.2. Georeferencing

Image georeferencing is defined by a transformation between the image coordinates specified in the camera frame and the geodetic (mapping) reference frame [25]. This process requires knowledge of the camera calibration and exterior orientation parameters; these last obtained in post-processing from the GPS/INS-derived trajectory. If they are not recorded during flight (i.e. no INS data available), they must be determined from traditional aero triangulation (AT). This is the process by which the spatial position and orientation of a photograph is determined based on the photogrammetric measurements of the images of ground control points appearing in the photographs [26]. AT also produces many control points and requires image matching, which might be very difficult for large-scale images of urban areas, no texture images, steep slopes or moving objects.

These problems are naturally avoided if direct georeferencing is used [4], thus, the GPS/INS approach can render in a dramatic reduction in the number of control points and might eventually lead to the elimination of AT.

3.3. Attitude determination

Exterior orientation solution was implemented with a strapped-down inertial measurement unit [27]. It works together with a control loop that maintains a stabilized platform with constant nadir pointing and heading [17]. This system works independently from the aircraft and the sensors are firmly attached to the fuselage. The inertial system is based on the utilization of gyroscopes and accelerometers in a complementary filter scheme, where a vertical determination reference is obtained [28]. The gyros find the orientation, and the accelerometers correct the drift of the former [29]. Inertial sensors determine the attitude in the pitch and roll axis, while an electronic compass finds the heading. The precision is better than ± 1 [arc deg] for a period of at least four hours (see response curves at the end of section 3.4)

3.3.1 Two-axis vertical determination

The knowledge of the angular attitude of an airborne platform with respect to an external reference axis system is of paramount importance in the realization of attitude estimation and control [28]. The typical quantities to be measured are the vehicle attitude Euler angles $\Phi,\Theta,$ and $\Psi$, defined with respect to the local level and local North, and the inertial vehicular angular rates P, Q, R. These quantities are depicted in figure 5. The rotation matrix performs the transformation of any vector from Earth axis Xe, Ye, Ze to body axis $X_b$, $Y_b$, $Z_b$. It is important to note that the inertial angular rates P, Q, R are not identical with the Euler angular rates $\dot{\Phi},\dot{\Theta},\dot{\Psi}$. The first triplet represents the projections of the total inertial angular rate vector $\Omega$ on the vehicle body axis $X_b$, $Y_b$, $Z_b$ while the later

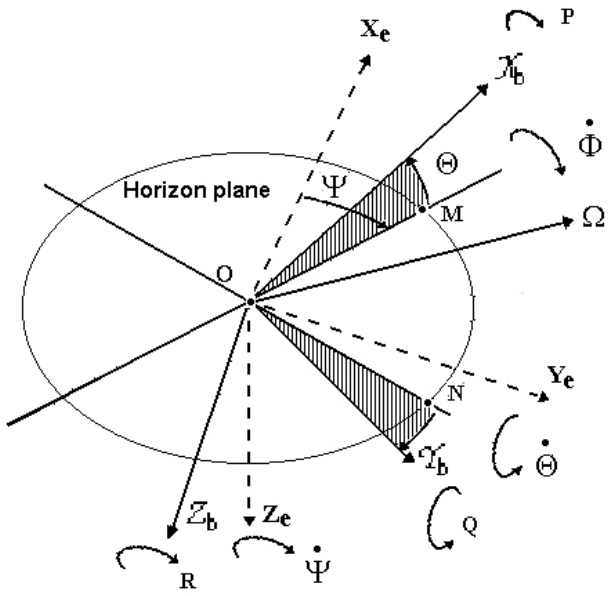


*Figure 5. Relationship between body axis and Earth axis.*

triplet represent the Euler angular rates around the axis *OM, ON* and *Ze,* respectively. The kinematical relationships between P, Q, R and $\dot{\Phi},\dot{\Theta},\dot{\Psi}$ are known as the Euler differential equations [30]:

$$\boldsymbol{P} = \dot{\Phi} - \sin\Theta \tag{1}$$

$$\boldsymbol{Q} = \dot{\Theta}\cos\Phi + \dot{\Psi}\cos\Theta\sin\Phi \tag{2}$$

$$\boldsymbol{R} = -\dot{\Theta}\sin\Phi + \dot{\Psi}\cos\Theta\cos\Phi \tag{3}$$

Alternatively, solving for $\dot{\Phi},\dot{\Theta},\dot{\Psi}$ in terms of P, Q, R yields

$$\dot{\Phi} = \boldsymbol{P} + \boldsymbol{Q}\sin\Phi\tan\Theta + \boldsymbol{R}\cos\Phi\tan\Theta \tag{4}$$

$$\dot{\Theta} = \boldsymbol{Q}\cos\Phi - \boldsymbol{R}\sin\Phi \tag{5}$$

$$\dot{\Psi} = \boldsymbol{Q}\frac{\sin\Phi}{\cos\Theta} + \boldsymbol{R}\frac{\cos\Phi}{\cos\Theta} \tag{6}$$

The last three nonlinear equations are of particular technical importance because they permit the computation of the Euler angles $\Phi$, $\Theta$, $\Psi$ given their initial conditions $\Phi_0$, $\Theta_0$, $\Psi_0$ and using the measurements P, Q, R; the angular velocities given by the gyroscopes in the pitch, roll and yaw axis respectively. The integrations of $\dot{\Phi},\dot{\Theta},\dot{\Psi}$ yield the computed Euler angles $\Phi_c$, $\Theta_c$, $\Psi_c$, which are referred to inertial space. These calculated values, accumulate errors due to Earth's rotation and gyro drifts. However, in the two-axis vertical determination system implemented, the accelerometers correct the gyro drift through an aiding scheme. Figure 6 shows the gravity-aided attitude reference system, the sub-indexes *m* and *c* are indicating measured and calculated quantities, respectively.

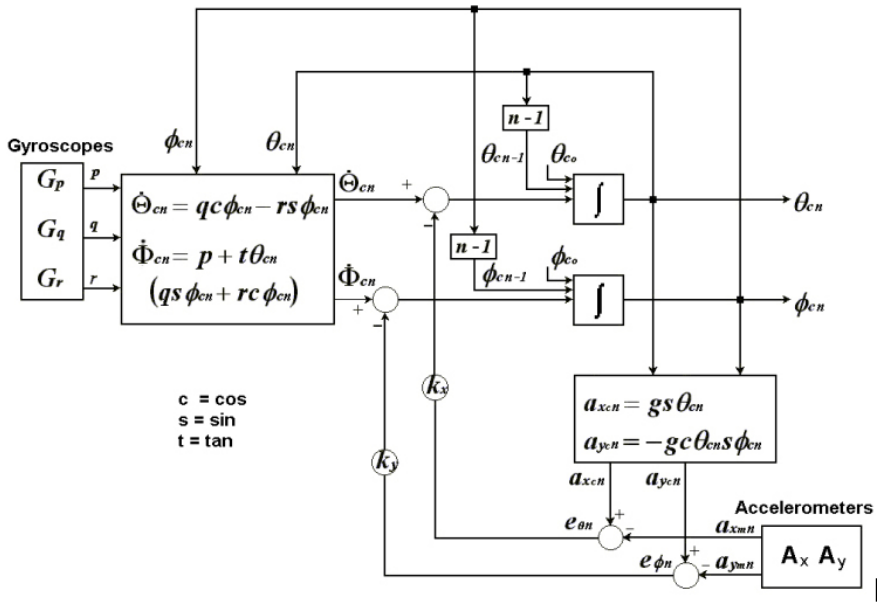


*Figure 6. Inertial determination scheme implemented to obtain a vertical reference.*

We are departing from:

$$\dot{\Theta}_c = \boldsymbol{q}\cos\phi_c - \boldsymbol{r}\sin\phi_c \tag{7}$$

$$\dot{\Phi}_c = \boldsymbol{p} + \tan\theta_c(\boldsymbol{q}\sin\phi_c + \boldsymbol{r}\cos\phi_c) \tag{8}$$

The $A_x$ and $A_y$ accelerometers mounted with its sensitive axis aligned with the pitch and roll axis are used to correct the $\theta_c$ y $\phi_c$ values. Measured accelerations $a_{xm}$ and $a_{ym}$ give tilt angle information of $\theta$ and $\phi$, these readings are compared with calculated accelerations $a_{xc}$ and $a_{xc}$. The difference between them is the error signal used to correct $\theta_c$ and $\phi_c$ through the constants $K_x$ and $K_y$.

$$\boldsymbol{a}_{xc} = \boldsymbol{g}\sin\theta_c \tag{9}$$

$$\boldsymbol{a}_{yc} = -\boldsymbol{g}\cos\theta_c\sin\phi_c \tag{10}$$

Finally we can determine $\theta_c$ and $\phi_c$ values from the following equations:

$$\theta_c = \theta_{c0} + \int_0^t [\boldsymbol{q}\cos\phi_c - \boldsymbol{r}\sin\phi_c - \boldsymbol{K}_x\boldsymbol{e}_\theta]\boldsymbol{dt} \tag{11}$$

$$\phi_c = \phi_{c0} + \int_0^t [\boldsymbol{p} + \tan\theta_c(\boldsymbol{q}\sin\phi_c + \boldsymbol{r}\cos\phi_c) - \boldsymbol{K}_y\boldsymbol{e}_\phi]\boldsymbol{dt} \tag{12}$$

In all the expressions of figure 6, a suffix *n* has been added in order to make a distinction between old and new variables. During algorithm execution integration time is computed from a C Language function, because time differences between data samplings were found, causing inconsistencies in the attitude determination [31]. Constants $K_x$ and $K_y$ where calculated empirically with $\theta_c$, $\phi_c$ and $a_{xm}$, $a_{ym}$.

3.4. Attitude determination and control stabilization.

The main components of the attitude determination and control system are showed on figure 7.

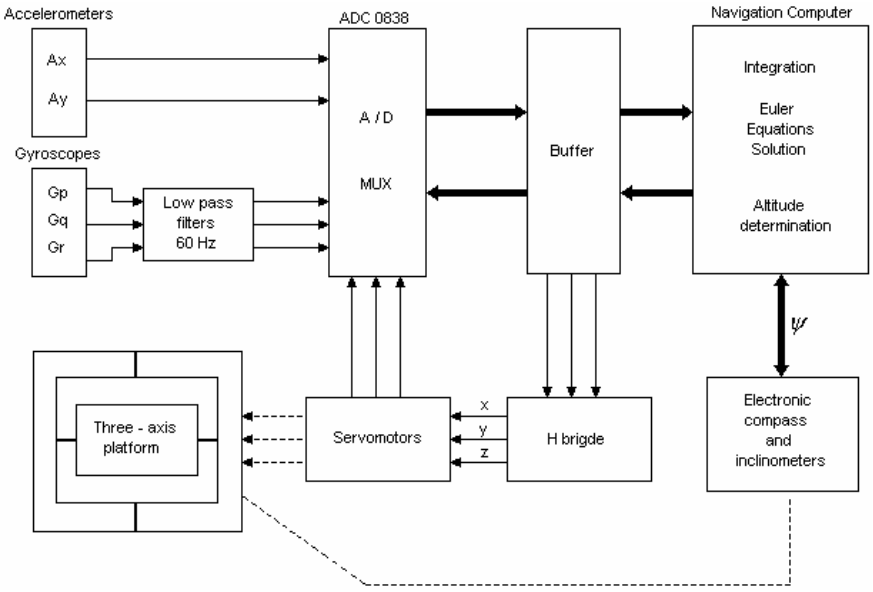


*Figure 7. Attitude determination and control stabilization system*

3.4.1 Sensors

A low-cost combination of three gyroscopes and two accelerometers were integrated in an IMU (see figure 8). Micromachined accelerometers [32] with an operational range of ±2 G's, RMS noise level of 0.02 [g] with signal amplification, conditioning and temperature compensation modules were used. The gyroscopes are piezoelectric devices [33], with an operational interval of ±100 [°/s] and RMS noise level of 0.05 [°/s].

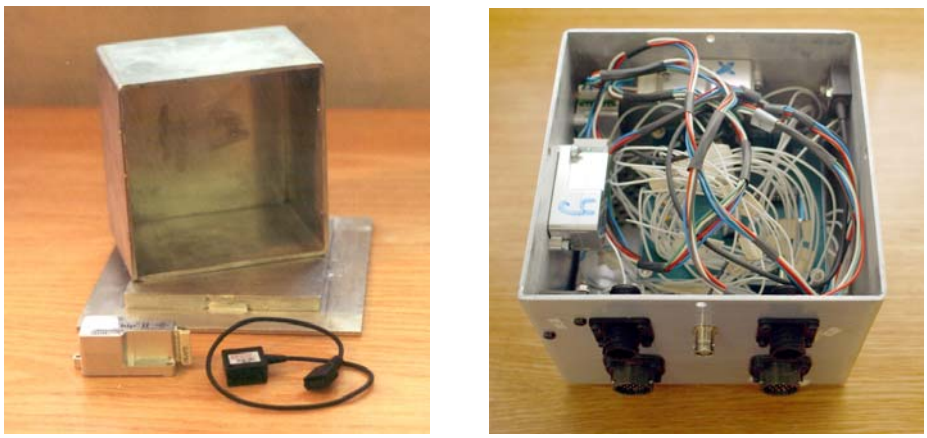

*Figure 8. Gyroscopes, and accelerometers are aligned with the axis of the IMU box.*

An electronic compass [34], composed by a three-axis magnetometer and two inclinometers, delivers yaw, and pitch and roll signals, respectively (see figure 9). This device outputs continuous azimuth (accuracy is ≤ 0.5 [arc-deg]), the three components of the magnetic field, dual axis tilt (for up to ± 80 [arc-deg] with an accuracy of 0.25 [arc-deg]), and temperature data. Serial communication is carried out through an RS232 interface. Inclinometers are employed to initially establish the horizontal reference for the IMU, before flight.

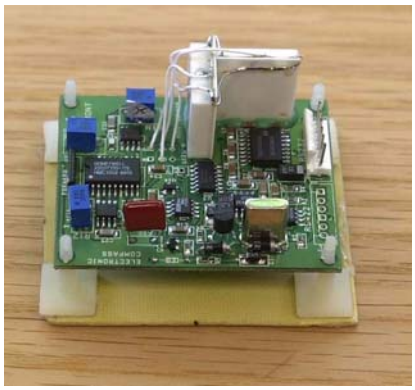

*Figure 9. Electronic compass for independent yaw determination*

Calibration curves of each sensor were obtained and introduced to the attitude algorithm for automatic compensation [31]. Gyroscopes, accelerometers, and inclinometers exhibit a linear response and were modeled with first order equations. Figure 10 shows two examples of the results of this calibration procedure, and figure 11 shows the response curves of the attitude system in three-axis.

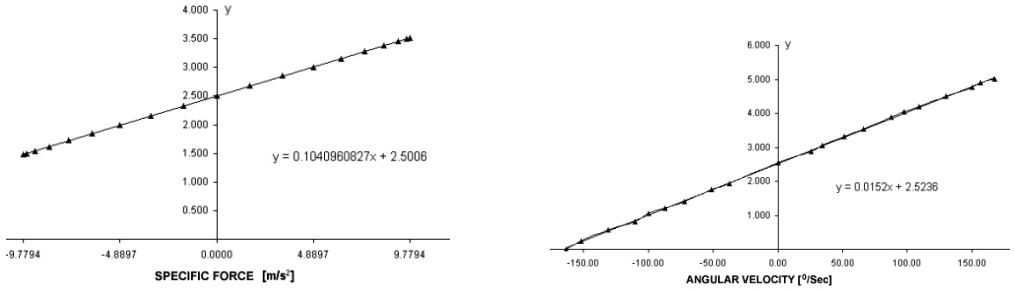


*Figure 10. Typical response curves for the accelerometers, and Gyroscopes, respectively.*

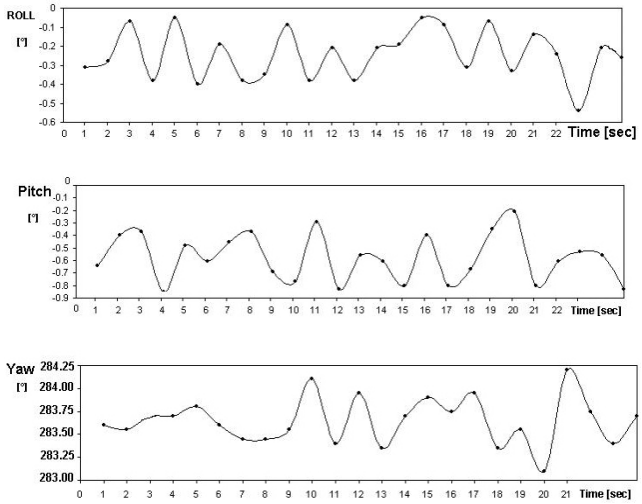


*Figure 11. Short-term response curves of the IMU (pitch and roll axis), and the electronic compass (yaw).*

3.4.2 Stabilized platform

Despite the six exterior orientation parameters determination, the utilization of a stabilized platform is recommended [17]. Involuntary movements and perturbations in the airplane during an aerial survey introduce significative

distortions into the images. The movement of the camera during exposure influences the quality/sharpness of the acquired imagery resulting in certain image blur [35]. To fully exploit the theoretical resolution power, forward motion compensation must be carried out by physically moving the sensor during image exposure. Additional rotational movements can be compensated from the stabilized mount. Such full motion compensation (translation plus rotation component) allows for a significant image quality improvement [35].

3.4.2.1. Platform mechanical design

Traditional CAD/CAM procedures were followed in the mechanical design and construction of the platform [36]. It consists basically of 6061-T6511 aluminum gimbaled frames with three degrees-of-freedom, a load capacity of 5.5 [kg], overall dimensions of 620 x 330 x 255 [mm], angular movements X=±20, Y=± 20, and Z=±42.5 [arc deg], and a total weight of 5.074 [kg]. Figure 12 shows an isometric view where the main components can be readily seen. Three DC motors (12 [volts] @ 0.5 [A]) are employed as actuators, driven by an H-bridge in a feedback servo control system interfaced thought the parallel port of the control and orientation PC.

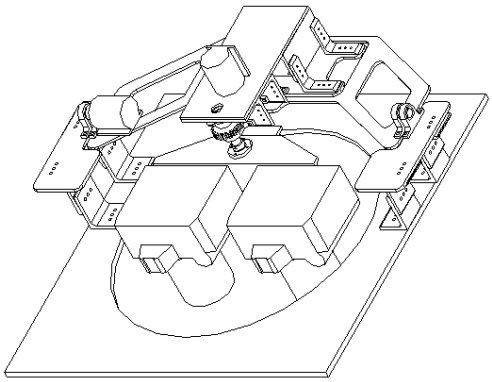

*Figure 12. Isometric view of the stabilized platform, capable of driving two cameras, usually one in color and one IR.*

Figure 13 shows a control test where an intentional deviation in the three-axis, at the same time, was induced. It is supposed to be the worst scenario the control system could face during a survey. The system exhibits a very fast and adequate response, taking into account the magnitude of the deviations.

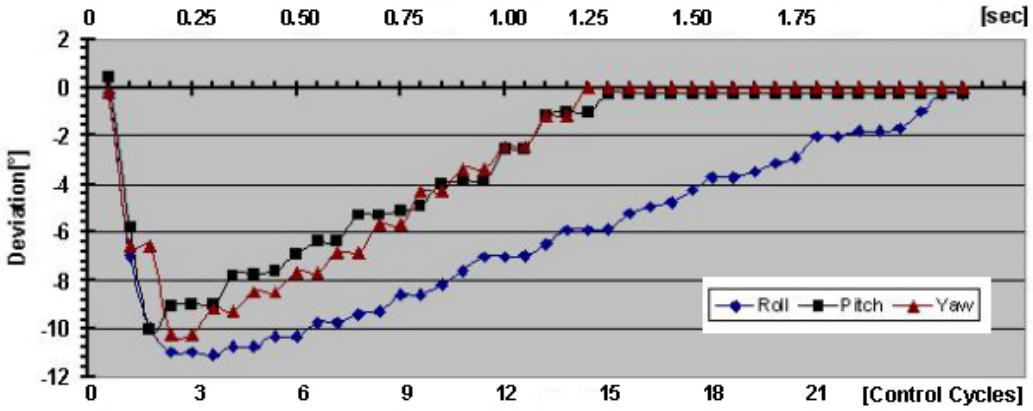


*Figure 13. Response curves after a perturbation was induced in the three-axis, simulating a critical condition.*

Laboratory and flight tests were carried out with the platform, figure 14 shows all the data handled by the attitude determination and control system. Real-time angular velocity of gyroscopes, specific force of accelerometers, angular position of the servomechanisms, orientation algorithm solutions, local gravity, and inclinometer attitude data are all displayed in real-time. This information is crucial for algorithm analysis and system performance evaluation.


*Figure 14. The real-time status of the attitude determination and control system is continuously displayed.*

The system is capable to maintain the orientation given by the IMU without noticeable error accumulation, which means that the accelerometers are effectively correcting gyro drift.

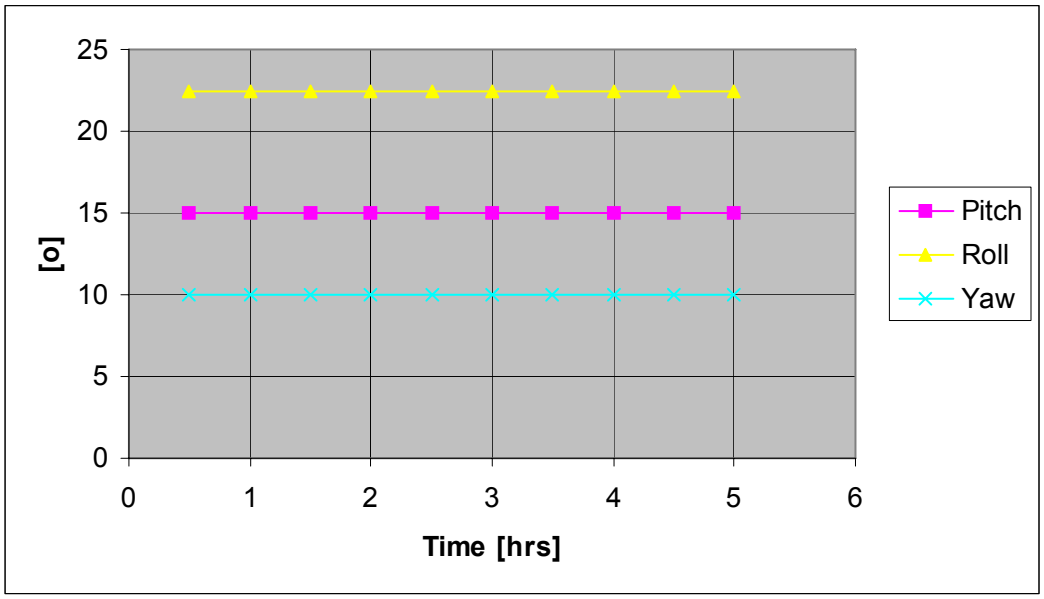


*Figure 15. Long-term response curves of the IMU (roll and Pitch) and the electronic compass (yaw).*

## 4. CAMERA CALIBRATION AND MOSAIC FORMATION

In order to maintain the low cost of our imaging system, the utilization of 35 mm SLR cameras is imperative[11]. Different cameras have been used in dozens of flight campaigns: Kodak DCS 420 (1524x1012 pixels), Nikon D1 (2012x1324), Nikon D1X (3000x2000), and Nikon D2X (4288x2848) in color. Three other were modified for IR acquisition: Kodak DCS 420 monochrome (1524x1012 pixels), SONY DSC-F707 (2560x1920), and Cannon EOS Revel (3456x2304). Additionally IR filters (i.e. B+W (87C) IR Glass filter), centered @ 910 [nm] and 100 [nm] wide in front of the lens, were used with very good results. Nowadays, high-resolution low-cost (6K USD) CCD or CMOS matrix sensors with 12 to 13 million pixels are readily available as a result of technological advances and professional photography demand. Nonetheless, the number of pixels is only one parameter that must be considered. Low-altitude flights require fast data transfer rates, and high-resolution demands high-quality lens. These are two fundamental constraints that must be considered for good quality imaging. Multispectral color imagery is obtained directly from the combination of the RGB channels and IR photographs, false color mosaics are very valuable, especially when vegetation assessment is performed.


*Figure 16. Small-format digital cameras: Kodak DCS 420 (1524x1012 pixels), and Nikon D2x (4288x2848)*

4.1. Camera calibration.

The calibration procedure is mandatory in small-format digital imaging systems to enhance image quality, and it is particularly important when photogrammetric work is being carried out [37]. Standard photogrammetric methods, similar to those used for calibrating metric cameras can be generally applied here [38]. It was expected that image geo-rectification would be more accurate if camera parameters were incorporated into the photogrammetric process and may be able to account for sources of random and systematic errors [38]. A traditional laboratory methodology was adapted for interior orientation parameter determination on small-format cameras. It is based in precise measuring of well-known points over an image, comparing its current location against the one they should have, if a perfect perspective was generated by the camera [25]. The optical axis deviation, the calibrated focal length, and the radial symmetric distortions of the lens are determined. An experimental arrangement was built in the laboratory with well-known distances, a regular squared pattern, and a fixed base for the camera (see figure 17). A squared grid of 10 [cm] was plotted, it is 90 [cm] wide and 1.5 [m] long, and the thickness of every line is 1 [mm].

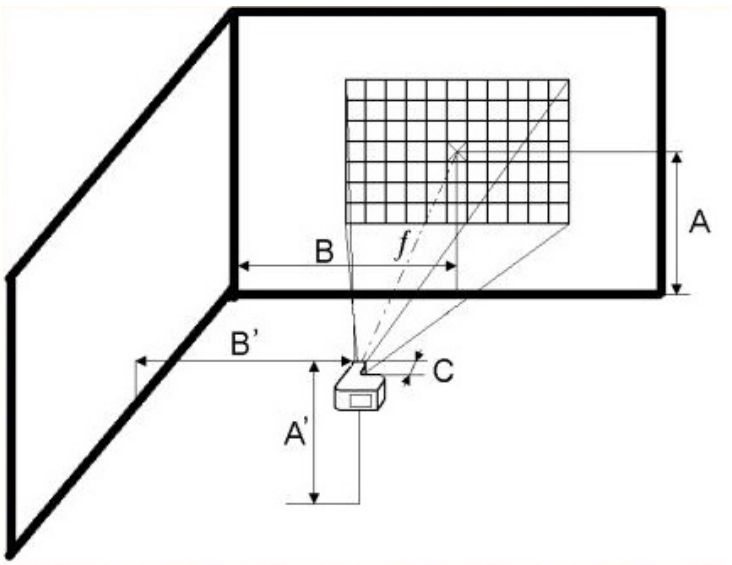


*Figure 17. Regular squared pattern and fixed station for camera calibration.*

With the camera focused at infinite one image is captured and then compared against the original pattern following eight lines crossing the center of the photograph (see figure 18). A set of 6 images is taken and the differences measured, averaged, and a table with radial distances vs. radial-lens distortions is created. With these data the coefficients of an adjusted polynomial curve, which models the symmetric radial lens distortion, are found.

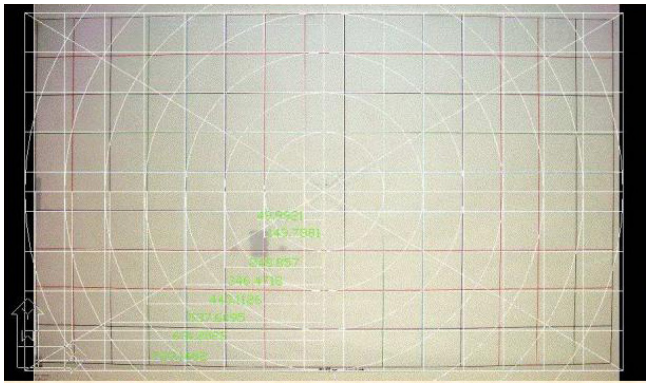

*Figure 18. Grid pattern superimposed over the image. The distances from the center and their corresponding distortions were measured.*

The polynomial is of the form:

$$\Delta r = k_1 r^1 + k_2 r^3 + k_3 r^5 + k_4 r^7 \tag{13}$$

Where $\Delta r$ is the lens symmetric radial distortion, $r$ is the radial distance from the principal point, and $k_1$, $k_2$, $k_3$ and $k_4$ are the coefficients of the polynomial that defines the shape of the distortion curve. Four $k$'s are necessary to obtain a unique solution, however, usually six measurements are made so, more than four equations are found and a least square method is well suited to determine the $K$ values.

The focal length is found through distance measurements and the application of the lens formula:

$$\frac{1}{o} = \frac{1}{i} = \frac{1}{f} \tag{14}$$

Where: $o$ is the object distance, $i$ is the image distance, and $f$ is the focal length.

4.2. Geometric distortion removal

An algorithm for geometric distortion removal was implemented, assuming that only symmetric radial distortion is present [15]. This procedure consists in the relocation of all of the elements of the image, after computing their new positions. The correction against principal point deviation is jointly applied with the lens distortion removal [25] (figure 19).

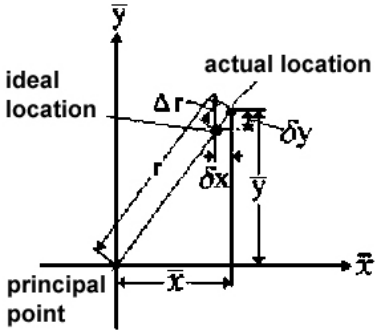


*Figure 19. Relationship between radial lens distortion and correction to x and y coordinates with respect to the principal point.*

In this way, all the pixels in the image are corrected determining its real position and finding the ideal one. Some cameras had been calibrated using this methodology; the image of figure 18 belongs to a SONY DSC-F707. This example demonstrates that some low-cost cameras introduce significant distortions, particularly towards the edges of the image (i.e. 31 pixels). RMS error after correction in this example is around 1 pixel. Another cameras tested, following the same procedure, were: KODAK DCS 420 (after the sensor was glued) and NIKON D1, D2X with errors ranging between 0.6 to 0.4 pixels. The difference is attributed to lens quality [37]. Figure 20 shows an example of the distortion removal process applied over aerial imagery obtained with the SONY DSC-F707.

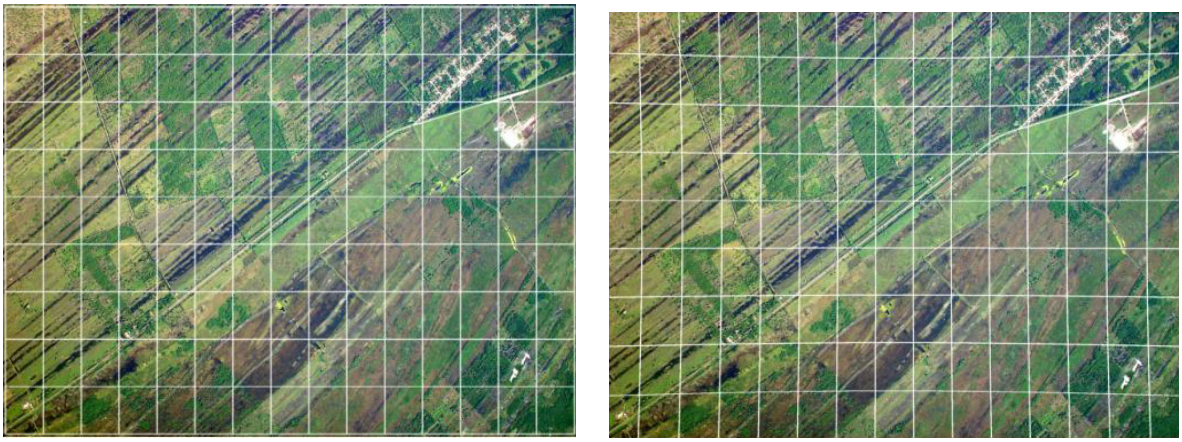

(a) (b)

*Figure 20. (a) Distortion removal procedure applied in an image with a regular squared pattern superimposed, and (b) corrected image.*

4.3. Image orthorectification and mosaic formation.

Orthomosaic construction is carried out using Erdas Imagine® software package. The GCP's are obtained from available orthorectified imagery and employed as georeference aid, and in some cases acquired through dedicated GPS campaigns. The GPS/INS data are processed to compensate for offsets between the IMU unit, the GPS antenna and the imaging sensors. GPS/INS interpolated geographical position and attitude data of each exposure station are used together with at least 9 ground control points per image to obtain the orthomosaic [39]. The system performance was evaluated with the external orientation parameters directly obtained from the GPS/INS, comparing the ground positions in the image with the GCP's in a flight over the valley of Mexico (figure 24). At an average image scale of 1:20,000 the achievable ground point positioning RMS accuracy is 8 [m]. The ASPRS planimetric feature coordinate accuracy requirement (ground X or Y) for well defined points [40], specifies that for a map scale of 1:10,000 the horizontal accuracy must be ± 7.5 [m] (class 3). Using this data the orthomosaic can be resampled to a map scale of 1: 10,600. This result demonstrates that with the system described here, orthomosaics fitting this standard can be obtained.

5. SYSTEM'S APPLICATIONS

This system has been used in many research projects, initially with a color camera and a hand-held GPS working in stand-alone mode; since then, it has been continuously evolving. In some cases image stereo-pairs are enough for interpretation and analysis, but the general requirement is the construction of the mosaic of the zone under study. As pointed out before, one of the most important aspects of the utilization of this technology is the relative short time between image acquisition and mosaic generation. This is particularly important in devastated zones, where quick assessment and response are indispensable for damage mitigation. In many cases 4 to 6 hours are enough for aerial photography coverage and mosaic construction (see figure 21).

Due to the high resolution that can be obtained on the ground, a very interesting application has been performed with this system: aerial sampling. In one project related with crop estimation [41], a 5 % error was obtained.

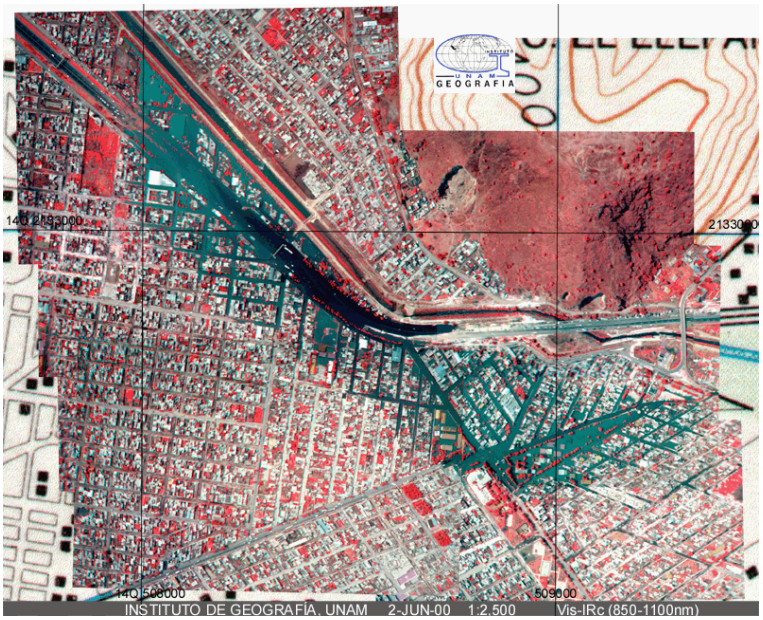


*Figure 21. Non-supervised digital mosaic created from visible and near IR digital images of the flooding of the densely populated area of Chalco, Mexico.*

Regarding the validation of the interpretation of vegetal coverage in Mexico [42], costly fieldwork was avoided. The monitoring software was modified to handle very large flight lines along and across de country [14]. Geographical coordinates were used in order to stay away from problems associated with changes between UTM zones. Almost two hundred flight-hours were spent in a Cessna 441 aircraft (figure 22) to cover the entire country

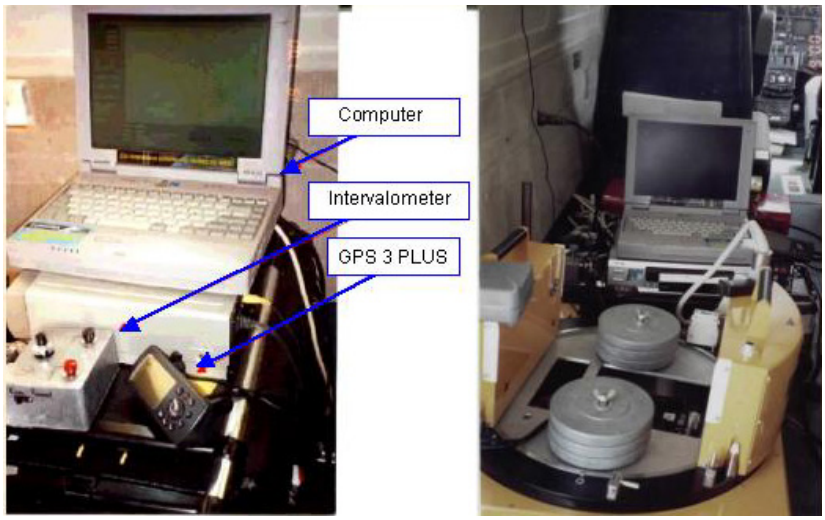


*Figure 22. Imaging system with the cameras mounted in the stabilized platform of a Zeiss RMK top aerial camera in a Cessna 441 aircraft.*

in a squared grid pattern of 50 [km] wide in the central and southern parts of the Mexican republic, and 100 [km] on the northern territory (see figure 23). A database containing 43,000 images was created with position information, date, time, focal length, and approximate scale [18,42].

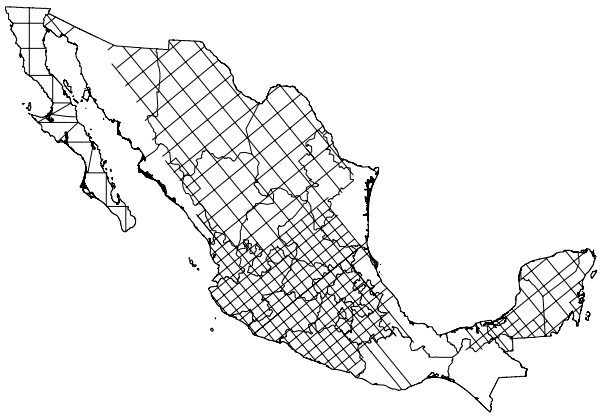

*Figure 23. High-resolution image sampling on transects along and across the Mexican Republic for validating the interpretation of the vegetal coverage.*

Figure 24 shows an aerial survey of the valley of Mexico. This example demonstrates, against the opinion of some authors [35, 43], that large area coverage can be performed with small-format digital cameras; the surface is 1,400 [$km^2$] approximately.

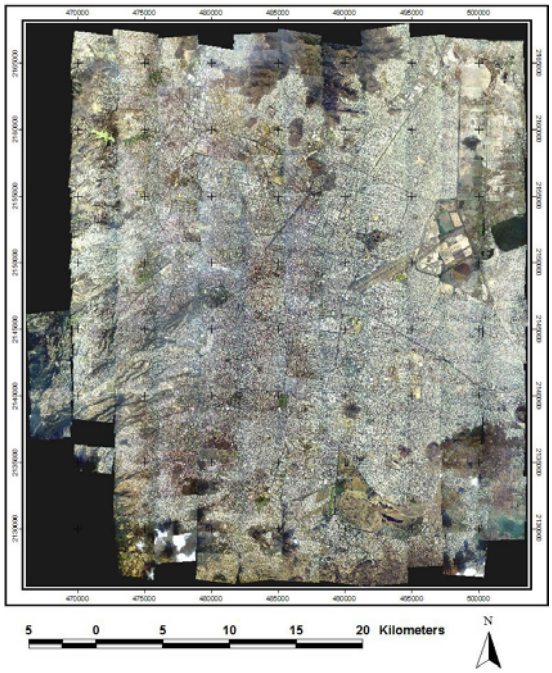


*Figure 24. Orthomosaic of the Valley of Mexico composed by 450 digital images.*

## 6. DISCUSSION

The INS accuracy degrades over time due to unbounded positioning errors caused by gyro drift affecting the INS measurements. On the other hand, the IMU must provide autonomous three-angle attitude determination with high short, and long-term accuracy. In the imaging system described here, low-cost rate sensors are employed, the drift in these piezoelectric gyros can reach 90 [°/hr], however, they are working in a gravity-aided scheme where attitude errors are bounded by the accelerometers, and short-term, as well as long-term accuracy is maintained. The concept of a complementary filter is widely employed in the integrated GPS/IMU systems developed in the last years [3,4,5,12,43,44,45], to improve position and attitude accuracy. Direct platform orientation can also be achieved by means of an array of GPS antennas, nonetheless, for the most demanding mapping applications this approach is not

able to provide acceptable EO parameters [4]. Combining DGPS and IMU data bounds the gyro drifts allowing for continuous IMU error calibration and positioning, however, such GPS/IMU components results in a significant price increase specially when using very-high quality products (i.e. Applanix POS/AV, IGI AEROcontrol) [35]. Table I shows the comparison of cost and accuracies achieved by some GPS/IMU sensors attached to different imaging systems, including the one described here. The accuracy in attitude determination an integrated GPS/INS system can provide, allows for direct georeferencing [12, 43, 44], and avoids costly GPC campaigns. This accuracy makes those systems suitable for cadastral or precise construction engineering projects, which demands sub-decimeter and at least 0.05 [arc-deg] in position and orientation, respectively [4]. These are the only two fields in which our system is limited.

*Table I. Characteristics of GPS/IMU sensors in some imaging systems.*

| System | GPS accuracy | IMU accuracy | Overall mapping accuracy | Camera cost USD | Total Cost USD |
|---|---|---|---|---|---|
| Applanix POS/AV | X=0.4, Y=0.05 Z=0.09 | $\omega,\varphi$=0.0085° $\kappa$=0.0152° | 0.3 - 0.5 [m] | $170K | $370K |
| AEROcontrol | < 10 [cm] | $\omega,\varphi$=0.005° $\kappa$=0.01° | Orthophoto production | N/A | $370K |
| AIMS | 4-7 [cm] | $\omega,\varphi$=0.0027° $\kappa$=0.0152° | 0.3 - 0.5 [m] | $15K | $370K |
| ADU5 (GPS with attitude determination) | 40 [cm] | $\omega,\varphi$=0.8° $\kappa$=0.4° | N/A | N/A | $18K 4 antenna array 1[m] separation |
| Vertical determination System (IGg) | 40 [cm] | $\omega,\varphi$=0.9° $\kappa$=1.1° | 8 [m] | $6K | $20K |

Considering point accuracy in object space, the utilization of small or medium-format digital cameras represent a drawback compared with large-format imagery (i.e. 36 Mpixels). The base-to-height ratio ($\vartheta$) of the sensor influences the object point determination. This value reflects the geometry during image recording and is one main factor for the resulting point accuracy in object space [35]. Since many of the small-format digital cameras are using wide-angle lens due to the virtual magnification of focal length caused by small size sensor arrays, this results in smaller ($\vartheta$) values and less object point accuracy. Moreover, the most common accommodation of the camera to augment the swat during an aerial survey is with the larger side of the sensor, oriented perpendicular to flight direction. This again influences the quality of photogrammetric point reconstruction. Some authors utilize one camera pointing directly to nadir and another oblique to strengthen the geometry [5]. This results in an improved accuracy by a factor of 2.3 when using stereo-pair processing.

These issues must also be considered when using small or medium-format digital cameras in an imaging system intended for photogrammetric purposes.

## 7. CONCLUSIONS

A low-cost high-resolution digital imaging system has been developed constituting a very valuable alternative remote sensing tool. Up to this date, more than 150,000 images has been obtained covering 300,000 [km$^2$] in 45 projects with scientific, government, and commercial purposes demonstrating that large area coverage can be performed using small-format cameras. The monitoring software contributes significatively to facilitate flight planning and management, allowing for supervision and storage of those critical variables of the survey. The inertial attitude system has long-term stability based on the utilization of a gravity-aided scheme, becoming in a drift-free behavior. The control system maintains the three-axis stabilized platform in the range of ± 1 [arc-deg], allowing for vertical photography acquisition. This condition is particularly advantageous at the moment of orthomosaic generation. A procedure following traditional calibration methods was developed for small-format camera interior orientation parameter determination. These data, together with the exterior orientation parameters, obtained from the GPS/INS system, are employed for orthomosaic construction.

The imaging system described here was developed to meet the challenge to assess natural resources management in a mega-diverse territory, obtaining multispectral imagery with high-spatial and temporal resolution in a practical and economical way. Ultimately, the requirements of scale and position accuracy are application dependent and this system posses enough flexibility to incorporate a wide variety of assignments. Orthomosaics obtained complies with mapping standards, broadening the spectrum of applications of the images, and giving the possibility to perform quantitative analysis.

## 8. REFERENCES

[1] Peralta-Fabi Ri., Peralta A., Prado J., Navarrete M., & Martínez W., The Development of a Digital Videogrametric Airborne System, SPIE Proc. Vol. 1943. State of the art photogrammetric mapping, pp 221-228. Orlando, Florida, USA. 1993.

[2] Everitt, J. H. & Escobar D. E., Using video imaging technology for remote sensing of natural resources. VII SELPER, pp.753-773. Pto. Vallarta, Jalisco, México. Nov., 1995.

[3] Cramer M., Stallmann D., & Haala N., High precision georeferencing using GPS/INS and image matching. Proc. Int. Symp. On Kinematic Systems in Geodesy, Geomatics and Navigation, pp. 453-462, Banff, Canada, 1997.

[4] Grejner-Brzezinska D.A., Direct exterior orientation of airborne imagery with GPS/INS system: performance analysis, Navigation, Vol. 46, No. 4, pp.261-270, 1999.

[5] Mostafa M. M. R., & Schwartz K.P., Digital image georeferencing from multiple camera system by GPS/INS. ISPRS J. of Photogrammetry & RS, Vo. 56, pp. 1-12, 2001.

[6] Mausel, P.W., Everitt J.H., Escobar D.E. and.King D.J., Airborne videography: current status and future perspectives. PE&RS, vol 58, pp. 1189-1195, 1992.

[7] King, D. J., Airborne multispectral digital camera and video sensors: a critical review of system designs and applications, Canadian J. of RS, pp. 245-273, 1995.

[8] King D., Walsh P. & Ciuffreda F., Airborne digital frame camera for elevation determination, PE&RS Vo. 60, No. 11, pp. 1321-1326, 1994.

[9] Mills J.P., Newton I. & Graham R. W., Aerial photography for survey purposes with a high resolution, small format, digital camera, Photogrammetric Record, Vo. 15, No. 88, pp. 575-587, October, 1996.

[10] Schwartz K. P., Chapman M. A., Cannon M. E. & Gong P., An integrated INS/GPS approach to the georeferencing of remotely sensed data, PE&RS, Vol 59, No. 11, pp. 1167-1674, 1993.

[11] Prado J. et al., Sistema de adquisición de imágenes aéreas digitales de alta resolución. SOMI XV Cong. Nac. de Instr., TEL 18, pp1-8. Guadalajara, Jalisco, México, 2000.

[12] Ip A.W.L., Mostafa M.M.R. & El-Sheimy N., Fast orthophoto production using the digital sensor system, Proc. of Map India, pp. 79-84, New Delhi, India. Jan. 28-30, 2004.

[13] Curtin, C., Geometric correction of airborne multi-spectral digital imagery, http://www.cage.curtin.edu.au/~geogrp/projspecimge.html, Sept., 2005.

[14] Bermúdez R., y Martínez U., Despliegue y almacenamiento de datos para un sistema de adquisición de imágenes aéreas. Tesis de Licenciatura, Facultad de Ingeniería, UNAM., pp1-116, Abril 16., 2001

[15] Hernández A., Corrección geométrica de imágenes aéreas digitales. Tesis de Licenciatura, Facultad de Ingeniería, UNAM., pp1-93, México, 2003.

[16] Prado J. et al., Implementación de un sistema de navegación inercial para orientación y control de una plataforma aérea. SOMI XV Cong. Nac. de Instr., pp1-6. Guad., Jalisco, México, 2000.

[17] Prado J, Peralta-Higuera A, Bisiacchi G & Palacio JL., 3-Axis Stabilized Platform and Monitoring System for Airborne Digital Imaging, ASPRS, 18th Biennial Workshop on CP&VRA., Work No. 33 pp 1-10. Amherst, Massachusetts, May 16-18, 2001.

[18] Palacio J.L. et al., La condición actual de los recursos forestales en México: resultados del Inventario Forestal Nacional 2000. Investigaciones Geográficas, Boletín del Instituto de Geografía, UNAM.,No. 43, pp. 183-202, 2000.

[19] Peralta-Higuera A. et al., The use of Digital Aerial Photographs in the Study of the Overwintering Areas of the Monarch Butterfly in Mexico, ASPRS, 18th Biennial Workshop on CP&VRA, pp 1-9, Amherst, Massachusetts, May 16-18, 2001.

[20] Peralta-Higuera A. et al., Aerial Digital Photography as a Tool for Watershed Management in Central Mexico, ASPRS, 18th Biennial Workshop on CP&VRA, pp 1-6, Amherst, Massachusetts, May 16-18, 2001,.

[21] Prado-Molina J., & Peralta-Higuera A., Diagnosis and Delimitation of a Natural Protected Area Using High-Resolution Multispectral Images. ASPRS, 20th Biennial Workshop on CPV&HRDIRA., pp. 1-7, Weslaco, Texas, Oct. 4-6, 2005.

[22] Prado J., Bisiacchi G, Peralta A., Bermúdez R., & Martínez U., Despliegue y almacenamiento de datos para un sistema de adquisición de imágenes. SOMI XIV Cong. Nac. de Instr., pp 633-637. Tonanzintla, Puebla, México. Octubre 4-8, 1999.

[23] Cornell G., Manual de Visual Basic 3 para windows, Mc-Graw Hill, 1994.

[24] TOPCON HiperL1/L2 GPS receiver. http://www.topcon.com

[25] Wolf P.R., & Dewitt B.A., Elements of photogrammetry with applications in GIS, Mc Graw-Hill, 2000.

[26] Zeng Z., & Wang X., A general solution of a closed-form space resection, PE&RS, Vol 58, No. 3, pp. 327-338, March, 1992.

[27] Prado J., Bisiacchi G., Sadovnitchii S., Rodríguez M., & Becerril J., Desarrollo de un sistema de navegación inercial del tipo sujeto al vehículo. SOMI XIV Cong. Nac. de Instr., pp 638-642. Tonanzintla, Puebla, México. Octubre 4-8, 1999.

[28] Merhav S., Aerospace Sensor Systems and Applications, Springer, New York, 1993.

[29] Bar Itzhack I.Y. & Ziv I., Frequency and time domain designs of a strap down vertical determination system. Proceedings AIAA Guidance, Navigation and Control Conference. Williamsburg, Paper 86-2149, 1986..

[30] Blakelock J.H., Automatic control of aircraft and missiles, Wiley, N.Y., 1991.

[31] Becerril J.M & Rodríguez M., Sistema de navegación inercial basado en giróscopos y acelerómetros. Tesis de Licenciatura, Facultad de Ingeniería, UNAM., pp1-85, México, 2000.

[32].- ICSENSORS Technical notes. Accelerometer model 3140. Milpitas, Cal. U.S.A., 1999.

[33].- SYSTRON DONNER GyroChip II Solid State Rotation Sensor. U.S.A., 1999.

[34].- ADVANCED ORIENTATION SYSTEMS Ez-Compass-3 Application Manual. Linden, NJ. USA., 1999

[35] Cramer M., Performance of medium format digital aerial sensor systems, Photogrammetric Week '05, Wichmann Verlag, Heidelberg. WG III/1, pp 1-6.

[36] Prado J., Pimentel L.E., Sandoval R., & Peralta-Higuera A., Airborne Stabilized Platform for Small-Format Digital Photography. ASPRS, 19th Biennial Workshop on CPV&AIRA, Logan, Utah, pp. 1-6, Oct. 6-8, 2003.

[37] Prado J., Hernández A. & Peralta-Higuera A., Small-Format Camera Calibration and Geometric Distortion Removal in Digital Aerial Images. ASPRS, 19th Biennial Workshop on CPV&AIRA. Logan, Utah, pp 1-6, October 6-8, 2003.

[38] Fuhr D., Dudka, M., Gage J.D., & Scarpace F., New approaches to georectification and image mosaicing in digital airborne imaging for agriculture, Final report, ERSC, Univ. of Winsconsin-Madison, pp1-15, 1999.

[39] Peralta-Higuera A. et.al. A Comparison of Small-format Digital vs. Metric Aerial Cameras for Medium to Large-scale Mapping. 20th Biennial Workshop on CPV & HRDIRA. Weslaco, Texas, USA. Oct. 4-6, pp1-6., 2005.

[40] ASPRS planimetric feature coordinate accuracy requirement for well-defined points.

http://www.usace.army.mil/usace-docs/eng-manuals/em1110-1-1000/c-2.pdf Sep. 2005.

[41] Torres V., Personal Communication, ORBIMAGE, Dulles, VA, USA.

[42] Mas J. F., Velásquez A., Palacio J. L., Bocco G., Peralta A., & Prado J., Assessing Forest Resources in Mexico: Wall-to-Wall Land Use/Cover Mapping. PE&RS, October, pp. 966-968, 2002.

[43] Heier H. & Hinz A., A digital airborne camera system for Photogrammetry and thematic applications. http://www.gisdevelopment.net/aars/acrs/1999/ts7 (acc. sep. 2005)

[44] Kremer J., & Kreuztal A.G., The integrated CCNS/AEROcontrol System: Design and results, http://www.ipi.uni_hannover.de/html/publikationen/special/oeepe_publ_no43, (accessed sept. 2005).

[45] Toth, Ch.K., Direct Sensor Platform Orientation: Airborne Integrated Mapping System (AIMS), International Archives of Photogrammetry and Remote Sensing, ISPRS Comm. III, Vol. XXXII, part 3-2W3, pp. 148-155, 1997.

AUTHORS BIOGRAPHY

**Jorge Prado-Molina.** Received his BSc. in 1983 from the University of Mexico, and his MSc. in 1993; both in electronics. Currently, he is pursuing an Eng. D. degree at the University of Mexico. His research interests are in the aerospace instrumentation area. He has participated in many research projects dealing with: payload integration, attitude sensors development, inertial measurement units, photogrammetric mapping systems, small satellites, and spacecraft simulators.

**Armando Peralta-Higuera.** Born in Mexico City in 1959. Graduated as a Biologist at the Universidad Autónoma Metropolitana in Mexico in 1986 and is pursuing an MSc degree at Faculty of Sciences at the University of Mexico. In 1997 co-founded the Alternative Remote Sensing and Advanced Technology Lab, at the Institute of Geography, University of Mexico, which he headed until 2005. In 1997 introduced in Mexico the use of small-format digital cameras as tools for remote sensing, and has since developed systems, methods and applications, aimed at increasing the availability of remote sensing data in planning, decision-making and assessment. His work includes the characterization of digital cameras and imagery, their validation as a source of information for large-scale and thematic mapping through photogrammetry, spectral analysis and integration with other data sources (GPS, LIDAR), the development of mechanisms, image acquisition systems, and their uses in different fields. He has applied these developments in a wide diversity of projects in natural resource assessment, conservation, environmental management and impact, ecological ordering, agriculture, natural disasters, urban studies and commercial projects.

**José L. Palacio-Prieto.** Geographer (National Autonomous University of Mexico, UNAM) with specialized courses in Watershed Management, GIS and Remote Sensing in the International Institute of Geoinformation and Earth Sciences (ITC) in the Netherlands. Fields of interest include Geomorphology (gully erosion), land use planning and land use and land cover change. He teaches geomorphology and GIS in the postgraduate program of Geography and works as researcher at the Institute of Geography-UNAM, where he was Director (1997-2004). He was appointed Vice President of the International Geographic Union for the period 2000-2004 and First Vice President for the period 2004-2008. In 2004 he was appointed as General Director of Postgraduate Studies of the UNAM.

**Rafael Sandoval-Vázquez..** Earned his BSc. in 2003 as electronics engineer from the University of Mexico. From 2001 to 2003 he was working in the development of an airborne digital imaging system. In the Last 3 years he has been specializing in computer systems security, promoting and applying the last innovations in this field, at the Engineering Faculty, UNAM. Since 2004 he heads the Computer Security Department. He is currently professor of the Computer Department and main author of the study programs for Security in Informatics in the Engineering Faculty at the University of Mexico.